

Spectroscopy with $\beta 2p$ and $\beta\text{-}\nu$ recoil shifts.

H.O.U. Fynbo^a L. Axelsson^b J. Äystö^a U.C. Bergmann^c
M.J.G. Borge^d L.M. Fraile^d A. Honkanen^e P. Hornshøj^c
Y. Jading^a A. Jokinen^f B. Jonson^b I. Martel^g I. Mukha^h
T. Nilsson^a G. Nyman^b M. Oinonen^a K. Riisager^c
T. Siiskonen^a M.H. Smedberg^b J. Thaysen^c O. Tengblad^d
F. Wenander^a and the ISOLDE collaboration^a

^a*EP Division, CERN, CH-1211 Genève 23, Switzerland*

^b*Experimentell fysik, Chalmers Tekniska Högskola och Göteborgs Universitet,
S-41296 Göteborg, Sweden*

^c*Institut for Fysik og Astronomi, Aarhus Universitet, DK-8000 Aarhus C,
Denmark*

^d*Instituto de Estructura de la Materia, CSIC, E-28006 Madrid, Spain*

^e*Helsinki Institute of Physics, University of Helsinki, P.O box 9, FIN-00014,
Finland*

^f*Department of Physics, University of Jyväskylä, FIN-40351 Jyväskylä, Finland*

^g*University of Huelva, Huelva, Spain*

^h*Institut für Kernphysik, Technische Universität, Darmstadt, Germany*

The beta-delayed proton emission from the lightest Ar-isotopes has been measured with a high-granularity, large solid-angle Si-detector set-up. Although designed for the detection of beta-delayed two-proton and three-proton events, the setup also permitted measurement of proton energy shifts due to the beta-neutrino recoil. We discuss how spectroscopic information can be extracted from such measurements, even at the drip line. For the case of ^{31}Ar , the ground state spin could be determined as $5/2$.

Key words: $^{31,32,33}\text{Ar}(\beta p, pp)$; measured $E_p(\theta_{\beta p})$; deduced angular-correlation parameters, nuclear spin J .

1 Introduction

The aim of this paper is to discuss new possibilities for obtaining spectroscopic information on states in nuclei far from the valley of beta-stability.

Beta-decays far from beta-stability are characterized by large Q_β -values and low separation energies in the daughters. Therefore, as the proton-dripline is approached, many of the states fed are particle unbound, and beta-delayed one- or two-proton emission becomes prominent [see the review in (1)]. The first part of this paper concerns implications of this situation for spectroscopy studies close to or at the proton-dripline.

In the second part of this paper, we discuss how the techniques developed for studying multi-particle final states at the dripline can be used to obtain spectroscopic information on unbound states fed in beta-decay.

For both parts we shall use the lightest isotopes of the element Argon for illustration. In Section 2, we first discuss the experimental setup used for obtaining the data to be discussed in Sections 3 and 4.

2 Experimental setup

The experimental data were obtained at the ISOLDE facility at CERN. The isotopes $^{31,32,33}\text{Ar}$ were produced in a CaO target by bombardment with 1 GeV protons. The mass-separated Ar^+ beams were subsequently directed to a measurement station consisting of a hemispherical mount holding 15 Si detectors and a double-sided 16×16 Si strip-detector. Due to the low energy of the ISOLDE beams, the produced isotopes could be stopped in a thin carbon foil in which the beta-particles and delayed protons deposit negligible energy. With a total geometric solid angle of 25% of 4π divided into 271 segments, this setup combines excellent efficiency with good angular resolution. All detectors had a thickness of $300 \mu\text{m}$, thus the majority of the beta-particles deposited less than 500 keV in the detectors, and separation between beta-particles and protons was not a problem. Due to quite high thresholds of the order of 200-500 keV, the detection efficiency for beta-particles was low: only 1-10% of the potentially observable beta-particles were recorded by the acquisition system. The internal energy calibration was based on the strongest proton lines from $^{32,33}\text{Ar}$. The yield for the dripline nucleus ^{31}Ar was 2-3 atoms/s, rising roughly two- and three- orders of magnitude for ^{32}Ar and ^{33}Ar respectively. Detailed information about the experimental setup can be found in (2). For the implications on the data acquisition system using this many channels, see (3).

3 Spectroscopy at the proton drip-line

Decay studies for neutron deficient nuclei have played an important role in clarifying beta-decays of Fermi type. This is because, for nuclei with $Z > N$, the isobaric analog state (IAS) in the daughter can be fed in the decay, whereas, for nuclei with $N > Z$ the Coulomb displacement energy moves the IAS out of the Q_β window. For the study of the Gamow-Teller part of the beta-decay, nuclei with $Z > N$ are also more interesting since, in analogy with the Fermi part, the main part of the strength is here energetically accessible. Close to the drip-line the states fed are particle unbound and emit protons which can be easily detected. The close correspondence between the proton energy and the position of the unbound state allows for studies of the Gamow-Teller strength distribution. A good discussion of the physics interest in such studies can be found in (5). In the remaining part of this section we discuss the special problems encountered when beta-delayed two-proton emission ($\beta 2p$) become prominent. Details on the discussion on the mechanism of $\beta 2p$ from this experiment can be found in (4).

The $\beta 2p$ decay mode was discovered at the Lawrence Berkeley Laboratory in the early eighties in the decays of ^{22}Al (6), ^{26}P (7) and ^{35}Ca (8) (see (9) and (10) for reviews of this pioneering work). Since then, a number of cases have been studied at GANIL: ^{22}Al (11), ^{23}Si (12), ^{27}S (13), ^{31}Ar (13; 14), ^{43}Cr (15) and recently ^{35}Ca (16). At ISOLDE, the case of ^{31}Ar has been studied in a series of experiments (17; 18; 2), which are reviewed in (19). The occurrence of $\beta 2p$ decay is closely related to the fact that the IAS collects a large beta-strength at high excitation energy in the daughter. However, in the most recent of the ISOLDE studies, two-proton emission from states fed in Gamow-Teller decay was observed for the first time (2). Here we will emphasize the main implications of two-proton emission for decay spectroscopy found in that experiment.

First, in order to fully characterize such complicated decays with the low yields presently available for nuclei close to the dripline, one has to apply detector set-ups with large solid angle and many segments. By measuring the energy and position of both protons, one can reconstruct the full decay energy :

$$Q_{2p} = E_1 + E_2 + \frac{m_p}{m_r}(E_1 + E_2 + 2\sqrt{E_1 E_2} \cos \Theta_{2p}),$$

where m_p is the proton mass and m_r is the mass of the recoiling ^{29}P -nucleus (undetected). The quality of this reconstruction depends on the resolution with which Θ_{2p} can be measured, hence the need for a high segmentation of the setup. Also the detection efficiency for two-proton events depends quadratically on the number of segments. Finally, to distinguish different emission

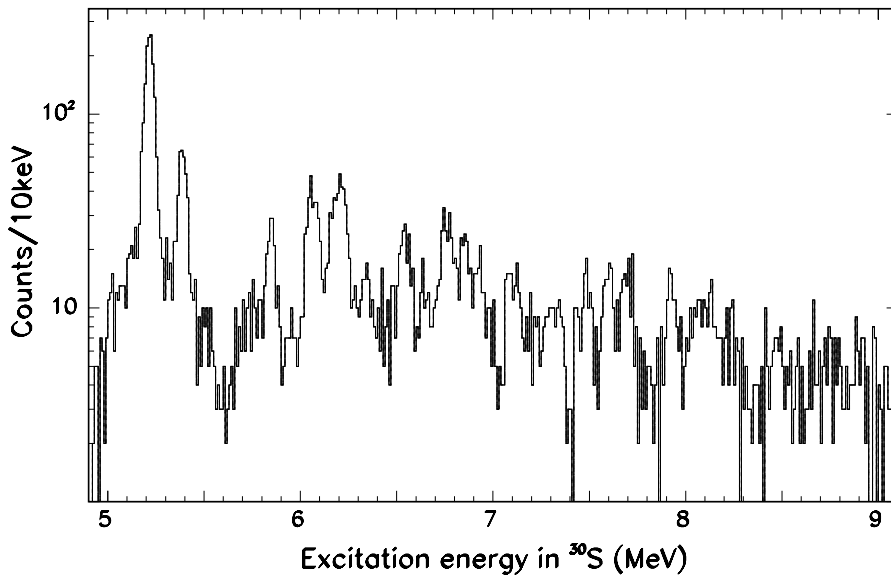


Fig. 1. Reconstructed spectrum of proton unbound states in ^{30}S fed from proton unbound states in ^{31}Cl in the beta-decay of ^{31}Ar . The energy of the ^{30}S states are calculated from Q_{2p} and from the energy of the first emitted proton in two-proton events in which both protons are detected.

mechanisms of the two protons, the setup must have a large angular acceptance (19).

For the decays of ^{22}Al , ^{26}P , ^{35}Ca and ^{31}Ar the $\beta 2p$ decays have been shown to proceed sequentially through narrow intermediate states in the respective intermediate nuclei. If the final state in the $\beta 2p$ is known, the position of the intermediate state can be calculated from Q_{2p} and the energy of the first emitted proton. Figure 1 shows the result of this procedure for the case of the decay of ^{31}Ar . The information on unbound states in ^{30}S obtained in this way is comparable to, or better than, that obtained from reaction studies with stable nuclei.

Since the two protons are emitted sequentially, they will give rise to peaks in the spectra of individual protons. In order to distinguish safely between protons belonging to one-proton and two-proton events it is therefore also required that the two proton events are well measured. In figure 2 we show the individual proton spectra from one-proton events and from two-proton events (shaded), where the later has been rescaled to take into account the difference in detection efficiency for events with one and two hits. Clearly some of the peaks observed in the individual proton spectrum are related to the two-proton events and should be assigned to the corresponding proton unbound states in ^{30}S . In the most precise previous measurement of this decay all peaks were assigned to bound states in ^{30}S (18).

As the final comment in this section, we note that the two-proton emitting

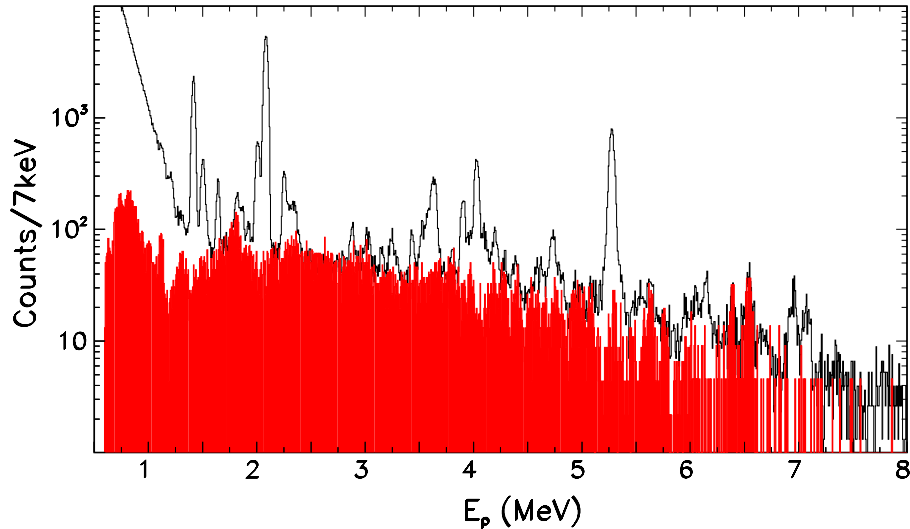


Fig. 2. The individual proton spectra from one-proton events and from two-proton events (shaded). The spectrum from two-proton events has been rescaled to take into account the difference in detection efficiency for events with one and two hits. Note that several of the peaks in the one-proton spectrum are explained by the two-proton events.

states are extremely important to include in the extraction of the Gamow-Teller strength. For the case of ^{31}Ar the total branching ratio to two-proton emitting states is close to 12 %, but, since these states are at high excitation energy, the corresponding Gamow-Teller strength ($B_{GT}=3.0(2)$), constitutes the main part of the observed strength.

4 Spectroscopy using the β - ν recoil shift

In most previous studies of beta-delayed proton emission, the presence of the beta-particle is considered a problem. This is because, with unsegmented detectors, a large solid angle will lead to a large probability for beta summing, which significantly reduces the quality of the proton spectra. With conventional detectors, taking beta-gated spectra leads to a reduction in statistics by 1-2 orders of magnitude, which cannot always be afforded far from stability. With highly segmented detector setups, the situation is reversed. Since each detector segment has a very small solid angle, the summing probability is negligible, and, due to the large number of segments, the difference in detection efficiency for events with one and two hits is strongly reduced. In the remaining part of this paper, we discuss how detecting the beta-particle in coincidence with the delayed particles can even be used to extract spectroscopic information. The results presented here have been published in (20), and more details can be found in (21).

The emission of the $\beta - \nu$ pair leaves the beta-daughter nucleus recoiling with a small energy, of the order 100 eV to 1 keV. In beta-delayed particle emission this recoil will be transferred to the delayed particle with an enhancement factor roughly equal to the ratio between the momenta of the emitted particle and the recoiling nucleus, often more than an order of magnitude. Since the higher energy and lower charge of the delayed particle reduces the sensitivity to scattering and energy losses in the source material, it is an important alternative to measuring the daughter recoil directly. Beta-recoil has been observed with delayed alpha-particles from ${}^8\text{Li}$ (22; 23) and ${}^{20}\text{Na}$ (24; 25; 26), delayed neutrons from ${}^9\text{Li}$ (27), and delayed protons from ${}^{32,33}\text{Ar}$ (28; 29). For ${}^{8,9}\text{Li}$ and ${}^{32,33}\text{Ar}$, the line broadening of the delayed particle peaks were observed, for ${}^{20}\text{Na}$ also the angle and energy of the positrons were recorded in coincidence. Whereas most of these measurements aimed at studying properties of the beta-decay itself, Schardt and Riisager (28) demonstrated that also spectroscopic information, such as level spins and peak assignments, can be deduced from the recoil shift by measuring precisely the line shapes of the delayed proton peaks. Here we extend the ideas put forward in (28) to measurements of the recoil shift as a function of the $\theta_{p\beta}$ angle in the full range between 0° and 180° .

A detailed discussion of the formalism used to describe beta-recoil energy-shifts is given in (31). To lowest order, the kinematic shift $\langle t \rangle$ of a proton with kinetic energy E_p averaged over the direction of the unobserved neutrino and the energy of the beta-particle is (26; 20) :

$$\begin{aligned} \langle t \rangle &= -t_{max} \cos \theta_{p\beta} \left(\left\langle \frac{p_\beta c}{T_{\beta,max}} \right\rangle + \frac{A}{3} \left\langle \frac{p_\nu c p_\beta c}{E_\beta T_{\beta,max}} \right\rangle \right) \\ A &= \frac{g_V^2 B_F - (1/3 + (2/30)\tau\theta) g_A^2 B_{GT}}{g_V^2 B_F + g_A^2 B_{GT}} , \\ t_{max} &= \sqrt{2m_p c^2 E_p} T_{\beta,max} / M c^2 , \end{aligned} \tag{1}$$

where m_p and M are the masses of the proton and the beta-decay daughter nucleus, p_β and p_ν the momenta of the beta-particle and the neutrino, $T_{\beta,max}$ the maximum kinetic energy of the beta-particle, and $\theta_{p\beta}$ the angle between the proton and the beta-particle. The parameters τ and θ in the ‘‘effective asymmetry parameter’’ A depend on the spin sequence in the decay and can be found in (28; 31). The total relativistic energy of the beta-particles is E_β , g_V and g_A are the coupling constants for the vector and axial vector weak currents, and B_F and B_{GT} are the squares of the corresponding reduced nuclear matrix elements. The averages over unobserved quantities with the Fermi function and the beta-neutrino phase-space are performed numerically. We note, however,

that for transitions with very high beta-energy, $T_{\beta,max} \gg m_{\beta}c^2$, one has

$$\langle t \rangle \approx -t_{max} \cos \theta_{p\beta} \left(\frac{1}{2} + \frac{A}{3} \frac{1}{2} \right) . \quad (2)$$

In this limit, both averages become 1/2; for the transitions investigated here, the numerical averages lie in the range 0.51–0.56 and 0.51–0.52, respectively.

For given experimentally observed values of $\cos \theta_{p\beta}$, $\langle t \rangle$ depends on $T_{\beta,max}$ and on A . The former is directly determined by the excitation energy of the state fed in the beta-decay. One cannot always deduce this excitation energy from E_p , since the particle emission can take place also to excited states in the final nucleus. Thus, determining $T_{\beta,max}$ from recoil energy shifts can replace particle-gamma coincidence measurements for determining the final state. Once the location of the transition in the decay scheme is known, one can extract a value for A . Fermi-decays can then be distinguished from Gamow-Teller decays, and for the latter one obtains constraints on the spin-sequence in the decay (through τ and θ). Thus all relevant spectroscopic observables can in principle be determined from beta-recoil shift measurements.

Figure 3 shows the recoil shift for the IAS in ^{32}Ar and for the strongest single proton peak following the decay of ^{31}Ar . The solid line in Figure 3 are fits with the expression $\langle t \rangle = -\bar{t} \cos \theta_{p\beta}$. Extracted values of \bar{t} from three proton lines following the decay of ^{32}Ar , two lines following the decay of ^{33}Ar and two lines following the decay of ^{31}Ar are shown in figure 4. For ^{32}Ar and ^{33}Ar , the spin-sequences are well known and we show with closed symbols the theoretical energy shifts calculated from eq. (1). The theoretical energy shifts are clearly larger than the ones observed experimentally. We attribute this to the low detection efficiency for high-energy beta-particles. The energy loss is low and rather constant for beta-particles with kinetic energies above 1 MeV, but increases towards lower energies. This implies that we preferentially select low values of $p_{\beta}c$. The effect is to lower the effective value of $\langle p_{\beta}c \rangle$ and, simultaneous, to increase $\langle p_{\beta}c p_{\nu}c / E_{\beta} \rangle$. In a simple model, this may be simulated via an extra weighting factor of p_{β}^{-2} in eq. (1). This should reveal the qualitative trends, but cannot be expected to give quantitative results. Results from this simple model are shown in figure 4 as open symbols. The agreement with the data points is clearly better. We conclude that we understand the data in a qualitative way. The two strongest proton lines from the decay of ^{31}Ar can safely be assumed to originate from two low-lying states in ^{31}Cl with spin 5/2 for the lowest of the two states and 3/2 for the upper one (20). Since both states are fed in allowed beta-decays, the possible spin values for ^{31}Ar are 3/2 and 5/2. The predictions for the energy shift for these two spin values are marked in figure 4 by triangles and circles, respectively. Both the values for complete beta-detection and for the simple model are given. The large difference between the two spin values stems from the A -parameters, which

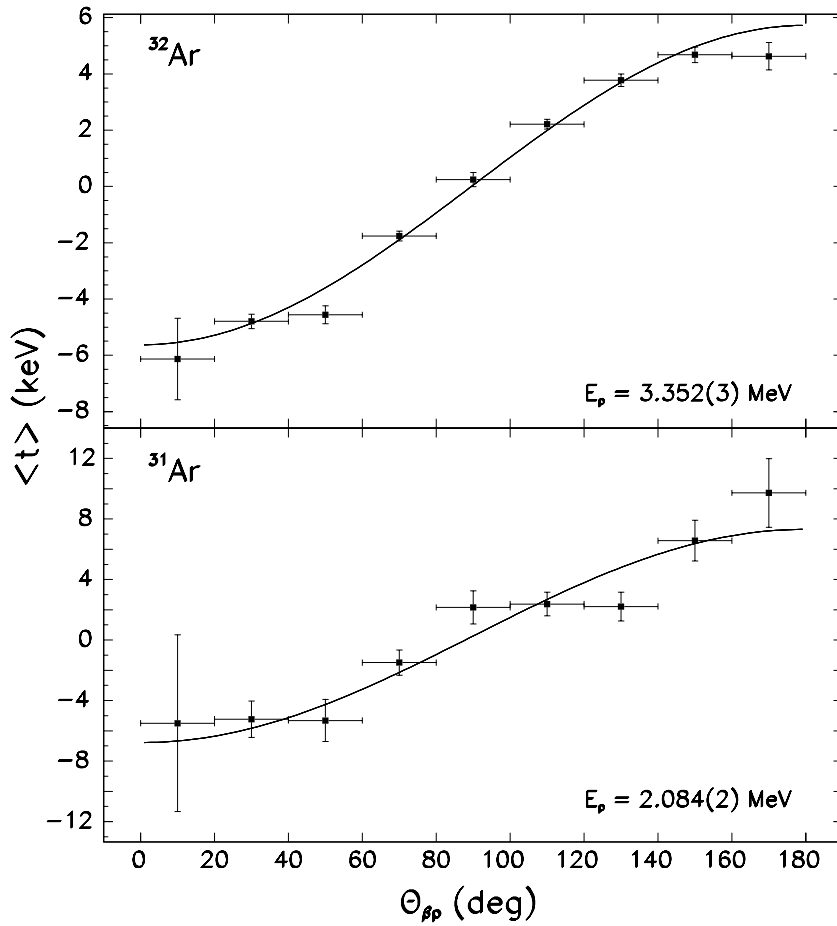


Fig. 3. The beta-recoil energy shift $\langle t \rangle$ is plotted versus the proton-beta angle $\theta_{p\beta}$. The solid lines are fits to the data. The top part is for the Fermi transition to the IAS in the decay of ^{32}Ar , the bottom part is for the Gamow-Teller transition to the second excited state in the decay of ^{31}Ar .

for the two lines are $1/5$ and $-13/15$ for spin $3/2$, and $-33/35$ and $-1/5$ for spin $5/2$. The data points clearly favour spin $5/2$. We note that this deduction is robust in the sense that we would need unphysical values of the effective averages $\langle p_\beta c \rangle$ and $\langle p_\beta c p_\nu c / E_\beta \rangle$ in order to reverse the conclusion.

5 Conclusions

We have shown that close to the proton drip line, where beta-delayed two-proton emission becomes prominent, highly segmented detector setups are required to fully characterize the final state. If the two-proton emission is sequential, spectroscopic information can be extracted on the intermediate states.

As a bonus, the highly segmented detector setups devised for this purpose

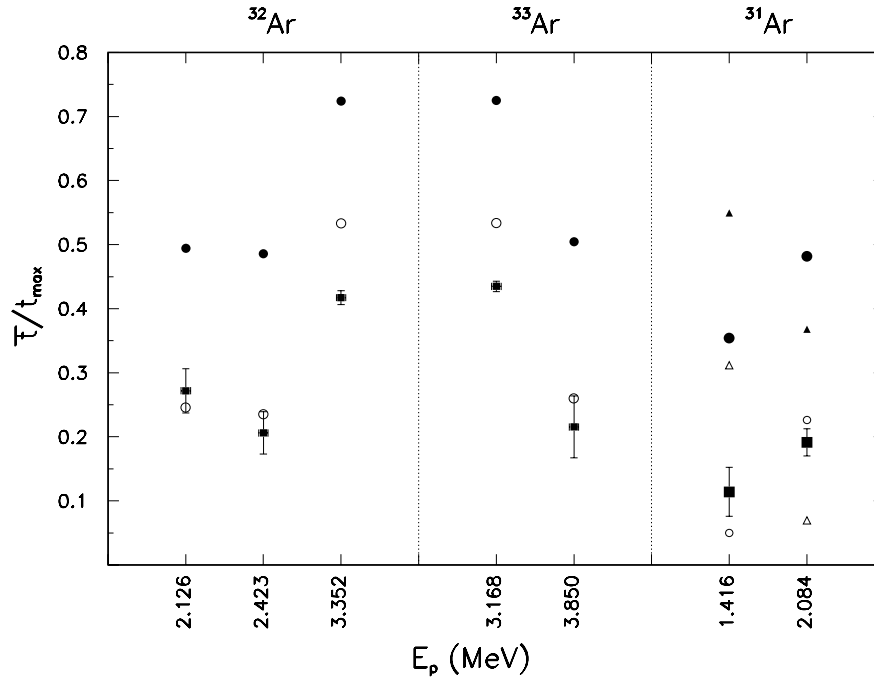


Fig. 4. The observed values of $\bar{\tau}/t_{max}$ from three proton lines following the decay of ^{32}Ar , two lines following the decay of ^{33}Ar and two lines following the decay of ^{31}Ar . The squares with error bars are the experimental values. The filled symbols are the theoretical values calculated directly from eq. (1), and the open symbols are from a simple model favouring detection of low energy beta-particles. For ^{31}Ar the triangles correspond to a spin of ^{31}Ar of $3/2$ and the circles to a spin of $5/2$.

strongly reduce the problem of beta summing. The beta-particle can be detected with high efficiency and, by analysing the recoil energy shift of beta-delayed proton lines, all relevant spectroscopic information can in principle be extracted. We have shown how the spin of ^{31}Ar could be determined in this way. Information on $T_{\beta,max}$ can be extracted readily, and may replace to otherwise needed gamma-particle coincidence measurements. Since such measurements far from stability are very difficult due to the low detection efficiency for gamma-rays, it is very important to find other means for correctly assigning particle spectra. If $T_{\beta,max}$ is known, one can determine A and, through this, in certain cases, spin values.

The two proton lines employed for ^{31}Ar gave each less than 1 proton/s in 4π . However, due to the efficient detectors with large solid angles and good granularity, clear results could be extracted. As the set-up was not optimized for this purpose, the detection efficiency for beta-particles was only about 10%. This should clearly be improved for future dedicated experiments.

References

- [1] B. Jonson and G. Nyman, in *Nuclear Decay Modes*, edited by D.N. Poenaru, Institute of Physics (1990), p. 102.
- [2] H.O.U. Fynbo *et al.*, Nucl. Phys. **A677** (2000) 38.
- [3] O. Tengblad *et al.*, these proceedings, Contribution 6/16.
- [4] M.J.G. Borge *et al.*, these proceedings, Contribution 10/5.
- [5] T. Björnstad *et al.*, Nucl. Phys. **A443** (1985) 283.
- [6] M.D. Cable, J. Honkanen, R.F. Parry, S.H. Zhou, Z.Y. Zhou and J. Cerny, Phys. Rev. Lett. **50** (1983) 404.
- [7] J. Honkanen, M.D. Cable, R.F. Parry, S.H. Zhou, Z.Y. Zhou and J. Cerny, Phys. Lett. **B133** (1983) 146.
- [8] J. Äystö, D.M. Moltz, X.J. Xu, J.E. Reiff and J. Cerny, Phys. Rev. Lett. **55** (1985) 1384.
- [9] J. Äystö and J. Cerny, in *Treatise on Heavy Ion Science*, Vol. 8, Nuclei Far from Stability, ed. by D. A. Bromley, Plenum Press, New York, 1989, p. 207-258.
- [10] C. Détraz and D. J. Vieira, Ann. Rev. Nucl. Part. Sci 39 (1989) 407.
- [11] B. Blank *et al.*, Nucl. Phys. **A615** (1997) 52.
- [12] B. Blank *et al.*, Z. Phys. **A357** (1997) 247.
- [13] V. Borrel *et al.*, Nucl. Phys. **A531** (1991) 353.
- [14] D. Bazin *et al.*, Phys. Rev. **C45** (1992) 69.
- [15] V. Borrel *et al.*, Z. Phys. **A344** (1992) 135.
- [16] W. Trinder *et al.*, Phys. Lett. **B459** (1999) 67.
- [17] M.J.G. Borge *et al.*, Nucl. Phys. **A515** (1990) 21.
- [18] L. Axelsson *et al.*, Nucl. Phys. **A628** (1998) 345.
- [19] M.J.G. Borge and H.O.U. Fynbo, Hyperfine Interactions **129** (2000) 97.
- [20] J. Thaysen *et al.*, Phys. Lett. **B467** (1999) 194.
- [21] J. Thaysen, Master thesis, Aarhus University, Unpublished.
- [22] K.H. Lauterjung, B. Schimmer and H. Maier-Leibniz, Z. Phys. **150** (1958) 657.
- [23] C.A. Barnes, W.A. Fowler, H.B. Greenstein, C.C. Lauritsen and M.E. Nordberg, Phys. Rev. Lett. **1** (1958) 328.
- [24] R.D. Macfarlane, N.S. Oakey, R.J. Nickles, Phys. Lett. **B34** (1971) 133.
- [25] E.T.H. Clifford *et al.*, Phys. Rev. Lett. **50** (1983) 23.
- [26] E.T.H. Clifford *et al.*, Nucl. Phys. **A493** (1989) 293.
- [27] G. Nyman *et al.*, Nucl. Phys. **A510** (1990) 189.
- [28] D. Schardt and K. Riisager, Z. Phys **A 345** (1993) 265.
- [29] A. Garcia *et al.*, Phys. Rev. Lett. **83** (1999) 1299.
- [30] V. Egorov *et al.*, Nucl. Phys. **A621** (1997) 745.
- [31] B.R. Holstein, Rev. Mod. Phys. **46** (1974) 789.
- [32] V. Borrel *et al.*, Nucl. Phys. **A473** (1987) 331.